JOINT INSTITUTE FOR NUCLEAR RESEARCH

Bogoliubov Laboratory of Theoretical Physics

# FINAL REPORT ON THE SUMMER STUDENT PROGRAM 2017

## Influence of the Coriolis interaction on the lifetime of isomeric states


**Supervisors:**
Prof. N.V. Antonenko
**Technical assistance:**
T.M. Shneydman

**Student:**
Markova Maria, Russia
Lomonosov Moscow State University


**Participation period:**
June 26 – August 6


Dubna 2017

# Contents

**Abstract**

The influence of the Coriolis interaction on the $N$-odd $Z$-even heavy and super-heavy nuclei rotational motion was investigated for isotones with $N = 149$:for the $^{243}$Pu, $^{245}$Cm, $^{247}$Cf, $^{249}$Fm, $^{251}$No, and $^{253}$Rf isotopes .The underlying theoretical base was derived. The treatment of basic single-particle energies was carried out in the framework of two-center shell model (TCSHM). For these isotones the corresponding E2 transition probabilities were evaluated in order to reveal the Coriolis item influence.

# 1 Introduction

The investigation of heavy and super-heavy nuclei structure became a subject of a particular relevant interest since the contemporary experimental techniques allowed to achieve an acceptable accuracy and to gain related spectroscopic data. There are some distinguished points on the general investigation path to the Island of stability – the isomeric states which,due to the long lifetimes, enable high-sensitively spectroscopic measurements in order to investigate both these states and decay-related ones [12]. The isomeric states and their population treatment reveals the crucial information on the related $\alpha-$decay chains rather than the ground states. Such long even directly measurable lifetimes are usually assumed to descend from the combination of large angular momentum and low transition energy. As long as a nuclear rotation tend to cause $K$ mixing of both isomeric and ordinary states, the theoretical picture for these states and their lifetimes which includes a mixing-causing addition (or a so called Coriolis interaction) is a grave frame for the heavy nuclei structure insight.

Since this problem was first set for the realm of heavy and super-heavy nuclei the appropriate theoretical framework was required. The macroscopic approaches are well developed and capable of gross structure description related to the collective nucleon motion. However they entirely omit some peculiar properties. Hence the selected approach should take some shell concerned details. Such unification was successfully developed in the microscopic-macroscopic approach. One if its most reliable and practical realizations for heavy and super-heavy nuclei was chosen in the present paper in order to construct a numerical base. As it was constructed to describe a wide variety of nuclear shapes during fission processes, its potential is split over two separate fragments which correspond to the different nuclear fragments. This model effectively reproduces the level spectra (spins and parities) with the respect to the internal model parameters. Therefore the description of particular nuclei as a concern of parametrization setting.

As long as the up-to-date experimental facilities enable to obtain an information on the heavy and super-heavy nuclei the theoretical results can be compared and jointly analyzed with the experimental data. Such modern spectroscopic techniques as in-beam spectroscopy, isomer spectroscopy, and decay spectroscopy have significantly enriched the experimental base on $N = 145, 147, ...157$ including the chain of $N$-odd $Z$-even isotones – $^{243}$Pu, $^{245}$Cm, $^{247}$Cf, $^{249}$Fm, $^{251}$No, and $^{253}$Rf [11]. The majority of spectroscopic data on $^{245}$Cm were obtained via $\alpha-$decay investigation [14, 15]. For $^{247}$Cf the experimental data [16] revealed the $7/2^+$ spin-parity of ground state and it was recently proved by its $\alpha-$decay on the excited $7/2^+$ state of $^{243}$Cm. The $\alpha-$decay of the $^{253}$No ground state $9/2^-$ allows to investigate the chain of decays of the $9/2^-$ excited states of $^{249}$Fm [17]. For the $^{251}$No isotope the spectroscopic data can be gathered both by $^{255}$Rf $\alpha-$decay and $^{m251}$No decay produced in heavy ions collisions [18]. However the $^{253}$Rf still one of the least investigated, there are just a few data sets available for it [13]. This isotonic line possesses the isomeric $1/2^+$ state with a lifetime varying from $0,29\mu$s to $1,02$s due to $5/2^+$ level below.This state if of particular interest in the scope of the Coriolis interaction.

# 2 Theoretical framework

Since the isotopes under investigation are odd nuclei with odd $N$ it is possible to apply microscopic-macroscopic rotor+particle model which distinguishes a valence neutron for a separate treatment. The equilibrium parameters of these nuclei ought to be evaluated via TCSHM application and the corresponding single-particle spectra must be taken into account for further Coriolis interaction involving.

## 2.1 Particle-plus-rotor approach

An exceptionally collective motion of nucleons can approximately reveal the general picture of the nucleus behavior in its vibrational or rotational motion. Single-particle features in a form of different transitions are entirely omitted in the collective models,though they are responsible for the shell structure revelation. Both of these models can be unified in order to consider single-particle and collective motion – the unified model which allows to split a nucleus into an inert rigid core (or a rotor) and a bunch of valence particles [4]. The elementary modification of this approach considers an odd nucleus and its division into an even-even inert core with an angular momentum $\vec{J}_{core} = 0$ and a valence nucleon with $\vec{J} = \vec{J}_{nucleus}$. So one may define the total angular momentum as:

$$\vec{I} = \vec{J} + \vec{R}, \tag{1}$$

where $\vec{R}$ denotes the total collective mechanical momentum. Such a consideration allows to divide the total Hamiltonian of this system into the intrinsic part which would correspond to the valence particle motion and the collective part for the core [2]:

$$H_{tot} = H_{int} + H_{col}. \tag{2}$$

As long as the collective part in the body-fixed system (1,2,3) is presented by:

$$H_{col} = \frac{R_1^2}{2\Theta_1} + \frac{R_2^2}{2\Theta_2} + \frac{R_3^2}{2\Theta_3}, \tag{3}$$

where $\Theta_i$ are the intrinsic components of the moment of inertia. The $R_i$ components can be easily excluded:

$$H_{col} = \frac{(I_1 - J_1)^2}{2\Theta_1} + \frac{(I_2 - J_2)^2}{2\Theta_2} + \frac{(I_3 - J_3)^2}{2\Theta_3} = \sum_{i=1}^{3} \frac{I_i^2}{2\Theta_i} + \sum_{i=1}^{3} \frac{J_i^2}{2\Theta_i} - \sum_{i=1}^{3} \frac{I_i J_i}{\Theta_i} =$$

$$= H_{rot} + H_{rec} + H_{cor}, \tag{4}$$

where $H_{rot}$ would correspond to the rotational movement of the core, $H_{rec}$ is the recoil component which would be automatically considered in the experimental values $\varepsilon_i$ in $H_{int} = \sum_i \varepsilon_i a_i^+ a_i$. As long as $[I_{x,y,z}, I_{1,2,3}] = 0$, rotational symmetry is not violated in the laboratory system, but it may be violated in the body-fixed one.

For the Hamiltonian the wave functions may be found in the form:

$$|\Psi_M^{iI}\rangle = \sum_K \Phi_K^i \, |IMK\rangle = \sum_K |\Psi_{MK}^{iI}\rangle \,, \tag{5}$$

where $\Phi_K^i$ is the efficient for the valence particle and $|IMK\rangle$ is the rotational collective efficient which is defined as the dependant on the Euler angles $\Omega$ normalized Wigner function:

$$|IMK\rangle = \sqrt{\frac{2I+1}{8\pi^2}} D_{MK}^I(\Omega) = N^I D_{MK}^I(\Omega), \tag{6}$$

The assumption of axial symmetry (internal 3 axis is the symmetry axis) would lead to $\Theta_1 = \Theta_2 = \Theta$, $R_3 = 0$, $I_3 = J_3 = K$, and the symmetrization must be considered as well:

$$|\Psi^{iI}_{MK}\rangle = \alpha_1 D^I_{MK}(\Omega)\Phi^i_K + \alpha_2 D^I_{M-K}(\Omega)\Phi^i_{-K}, \tag{7}$$

The rotation around both 2-axis and 1-axis in 3-axis symmetry case would lead to the same result, hence only 1-axis rotation $R^1$ can be considered by its dividing to the internal rotation $R^1_{int}$ (with the respect to 1,2,3 frame) and general rotation $R^1_{gen}$ $R^1 = (R^1_{gen})^{-1}R^1_{int}$ [8]:

$$R^1_{gen}D^I_{MK}(\Omega) = (-1)^{I-K}D^I_{M-K}(\Omega), \tag{8}$$

$$(R^1_{gen})^{-1}D^I_{MK}(\Omega) = (-1)^{I+K}D^I_{M-K}(\Omega), \tag{9}$$

$$R^1_{int}\Phi^i_K = \gamma\Phi^i_{-K}, \gamma = 1. \tag{10}$$

So, the primary wave function may be rewritten as:

$$|\Psi^{iI}_{MK}\rangle = \frac{1}{\sqrt{2}}(1 + (R^1_{gen})^{-1}R^1_{int})N^I D^I_{MK}(\Omega)\Phi^i_K = \frac{1}{\sqrt{2}}N^I D^I_{MK}(\Omega)\Phi^i_K +$$

$$+\frac{1}{\sqrt{2}}(-1)^{I+K}N^I D^I_{M-K}(\Omega)\Phi^i_{-K}. \tag{11}$$

If the Coriolis component is insignificant relatively to the the single-particle energy gaps, the valence particle follows the core rotations.The Coriolis contribution will be eliminated and the eigenvalues of the reduced Hamiltonian $H_{tot} = H_{int} + H_{rot}$ will be:

$$(E^{iI}_K)^0 = \varepsilon^{iI}_K + \frac{1}{2\Theta}(I(I+1) - K^2). \tag{12}$$

In order to apply the first order of perturbation theory it is rather convenient to modify the Coriolis component:

$$H_{cor} = -\sum_{i=1}^{3}\frac{I_i J_i}{\Theta_i} = -\frac{I_1 J_1}{\Theta} - \frac{I_2 J_2}{\Theta} = -\frac{(I_+ + I_-)(J_+ + J_-)}{4\Theta} - \frac{(I_+ - I_-)(J_+ - J_-)}{4\Theta} =$$

$$= -\frac{I_+ J_- + I_- J_+}{2\Theta_i} \tag{13}$$

Thus, the first order of perturbation theory provides us with:

$$(E^{iI}_K)^1 = (E^{iI}_K)^0 - \frac{1}{2\Theta}\langle\Psi^{iI}_{MK}|I_+ J_- + I_- J_+|\Psi^{iI}_{MK}\rangle, \tag{14}$$

which will stay the same value as the zeroth order of perturbation theory if $K \neq \frac{1}{2}$, otherwise it would have an additive item:

$$(E^{iI}_K)^1 = (E^{iI}_K)^0 - \frac{1}{2\Theta}(-1)^{I+\frac{1}{2}}(I + \frac{1}{2})\langle\Phi^i_{\frac{1}{2}}|J_+|\Phi^i_{-\frac{1}{2}}\rangle, \tag{15}$$

here $\langle\Phi^i_{\frac{1}{2}}|J_+|\Phi^i_{-\frac{1}{2}}\rangle$ the decoupling parameter. If the Coriolis component is not taken into account as a minor addition, the wave function may be rewritten as:

$$|\Psi^{iI}_{MK}\rangle = \sum_K \alpha^I_{MK}\Phi^i_K|KLM\rangle, \tag{16}$$

$$H_{tot}\sum_K \alpha^I_{MK}\Phi^i_K\,|KLM\rangle = E^I_M\sum_K \alpha^I_{MK}\Phi^i_K\,|KLM\rangle\,, \tag{17}$$

$$\sum_K \alpha^I_{MK}\,\langle\Psi^{iI}_{MK}|H_{tot}|\Psi^{iI}_{MK'}\rangle = E^I_M\alpha^I_{MK'}, \tag{18}$$

or in a matrix form:

$$\begin{pmatrix} H_{K_1K_1} & H_{K_1K_2} & \cdots & H_{K_1K_N}\\ H_{K_2K_1} & H_{K_2K_2} & \cdots & H_{K_2K_N}\\ \vdots & \vdots & \ddots & \vdots\\ H_{K_NK_1} & H_{K_NK_2} & \cdots & H_{K_NK_N}\end{pmatrix}\begin{pmatrix}\alpha^I_{MK_1}\\ \alpha^I_{MK_2}\\ \vdots\\ \alpha^I_{MK_N}\end{pmatrix} = E^{iI}_K\begin{pmatrix}\alpha^I_{MK_1}\\ \alpha^I_{MK_2}\\ \vdots\\ \alpha^I_{MK_N}\end{pmatrix} \tag{19}$$

where $K = \frac{1}{2}, \frac{3}{2}, ...$ and the matrix elements $H_{K_nK_m}$ in the case of $n = m$ are (for the detailed derivation see Appendix A):

$$H_{K_nK_m} = \begin{cases}\varepsilon^{iI}_K + \frac{1}{2\Theta}(I(I+1) - K^2), & \text{if } n = m,\ K \neq \frac{1}{2}\\ \varepsilon^{iI}_K + \frac{1}{2\Theta}(I(I+1) - \frac{1}{4}) - \frac{1}{2\Theta}(-1)^{I+\frac{1}{2}}\,\langle\Phi^i_{\frac{1}{2}}|J_+|\Phi^i_{-\frac{1}{2}}\rangle\,, & \text{if } n = m,\ K = \frac{1}{2}\end{cases}$$

And in the case of $n \neq m$ are:

$$H_{K_nK_m} = \begin{cases}\frac{1}{2}\sqrt{(I-K)(I+K+1)}\,\langle\Phi^i_K|J_-|\Phi^i_{K+1}\rangle - \frac{1}{2}\sqrt{(I-K)(I+K+1)}\,\langle\Phi^i_{-K}|J_+|\Phi^i_{-K-1}\rangle\,,\\ \text{if } m = n+1 \text{ or } n = m+1\\ 0,\\ \text{if } m = n+\delta \text{ or } n = m+\delta,\ \delta \in \mathbb{Z},\ \delta \gtrsim 2\end{cases}$$

The only parameter left for the further evaluation is a decoupling parameter which depends on the internal coordinates including valence particle coordinates and, if the vibrations are assumed in general, on the vibrational coordinates as well. Its sign and value denote the direction of a state shift and its scale correspondingly. The positive decoupling parameter would cause the downward removal of $I = 1/2, 5/2, ...$ states.

## 2.2 The two center shell model

In order to represent the single-particle wave function $\Phi^i_K$ to calculate decoupling parameters the asymmetric two center shell model [1] was used. This model enlarges the advantages and abilities of the Nilsson model to obtain the separate nucleus fragments to describe the pre-fission state (or an excited deformed state with no respect to fission). Its single-particle Hamiltonian can be rewritten in cylinder coordinates as:

$$H_{tc} = -\frac{\hbar^2\nabla^2}{2m_0} + V(\rho, z) + V_{LS}(\vec{r}, \vec{p}, \vec{s}) + V_{L^2}(\vec{r}, \vec{l}), \tag{20}$$

where $V(\rho, z)$ includes two-center-oscillator. Under some restrictions [1] the Shrödinger equation allows to divide a single-particle wave function (with no spinor taken into account):

$$\psi(\rho, z, \phi) = \mu(z)\chi(\rho)\eta(\phi), \tag{21}$$

where

$$\eta(\phi) = \eta_m(\phi) = \frac{1}{\sqrt{2\pi}}e^{im\phi} = |m\rangle\,,$$

$$\chi(\rho) = \chi_{n_\rho}^{|m|}(\rho) = N^{-1} k_\rho^{\frac{|m|+1}{2}} e^{-\frac{1}{2}k_\rho\rho^2}\rho^{|m|}L_{n_\rho}^{|m|}(k_\rho\rho^2) = |n_\rho\rangle\,,$$

$$\mu(z) = |n_z\rangle = \begin{cases} N_{z_1}^{-1}U(-n_{z_1}-\frac{1}{2}, -\sqrt{2k_{z_1}}(z-z_1) & \text{if } z<0 \\ N_{z_2}^{-1}U(-n_{z_2}-\frac{1}{2}, -\sqrt{2k_{z_2}}(z-z_2) & \text{if } z>0 \end{cases}.$$

Here $L_{n_\rho}^{|m|}$ is a Laguerre polynomial, $k_\rho = \frac{m_0\omega_\rho}{\hbar}n_\rho$, and $U$ is a parabolic cylinder function.It would provide us with a wave function form with a respect to the two-center-model quantum numbers $m, n_\rho, n_z$:

$$\psi(\rho, z, \phi) = |mn_\rho n_z\rangle\,|s\rangle\,, \tag{22}$$

As long as the framework is presented in the cylinder coordinates the acting ladder operators $J_+$ and $J_-$ ought to be rewritten in the same coordinates as well:

$$J_+ = ze^{i\phi}\frac{\partial}{\partial\rho} + i\frac{z}{\rho}e^{i\phi}\frac{\partial}{\partial\phi} - \rho e^{i\phi}\frac{\partial}{\partial z}, \tag{23}$$

$$J_- = -ze^{-i\phi}\frac{\partial}{\partial\rho} + i\frac{z}{\rho}e^{-i\phi}\frac{\partial}{\partial\phi} + \rho e^{-i\phi}\frac{\partial}{\partial z}, \tag{24}$$

Therefore the matrix elements $\langle\Phi_{K_i}^i|J_\pm|\Phi_{K_j}^i\rangle$ are in the form $\langle m_2 n_{\rho_2} n_{z_2} s_2|J_\pm|m_1 n_{\rho_1} n_{z_1} s_1\rangle$. A separated spin part $\langle s_2|s_1\rangle$ would provide with $\delta_{s_1 s_2}$. The angular parts in its explicit forms would are obtained as:

$$\langle m_2 s_2|J_+|m_1 s_1\rangle = -\hbar\left[(\rho\frac{\partial}{\partial z} - z\frac{\partial}{\partial\rho}) + \frac{zm_1}{\rho}\right]\delta_{s_1 s_2}\delta_{m_1 m_2 - 1}, \tag{25}$$

$$\langle m_2 s_2|J_-|m_1 s_1\rangle = \hbar\left[(\rho\frac{\partial}{\partial z} - z\frac{\partial}{\partial\rho}) - \frac{zm_1}{\rho}\right]\delta_{s_1 s_2}\delta_{m_1 m_2 + 1}, \tag{26}$$

The explicit form of $\langle m_2 n_{\rho_2} s_2|J_\pm|m_1 n_{\rho_1} s_1\rangle$ was derived as well. It is split to four different cases of $m_1$ and $m_2$ relations: the first case would correspond to $m_1 \geq 0$, $m_2 = m_1 + 1$ (and with the opposite sign the second case of $m_1 \leq 0$, $m_2 = m_1 - 1$):

$$\langle m_2 n_{\rho_2} s_2|J_+|m_1 n_{\rho_1} s_1\rangle = -\hbar[(\frac{1}{\sqrt{k_\rho}}\frac{\partial}{\partial z} + z\sqrt{k_\rho})\sqrt{n_{\rho_1} + |m_1| + 1}\delta_{n_{\rho_1} n_{\rho_2}} +$$

$$+(\frac{1}{\sqrt{k_\rho}}\frac{\partial}{\partial z} - z\sqrt{k_\rho})\sqrt{n_{\rho_1}}\delta_{n_{\rho_1} n_{\rho_2}+1}]\delta_{s_1 s_2}\delta_{m_1 m_2 - 1}, \tag{27}$$

and for $m_1 \geq 1$, $m_2 = m_1 - 1$ (with the opposite sign for $m_1 \leq -1$, $m_2 = m_1 + 1$

$$\langle m_2 n_{\rho_2} s_2|J_+|m_1 n_{\rho_1} s_1\rangle = \hbar[(\frac{1}{\sqrt{k_\rho}}\frac{\partial}{\partial z} - z\sqrt{k_\rho})\sqrt{n_{\rho_1} + |m_1| + 1}\delta_{n_{\rho_1} n_{\rho_2}} -$$

$$+(\frac{1}{\sqrt{k_\rho}}\frac{\partial}{\partial z} + z\sqrt{k_\rho})\sqrt{n_{\rho_1}}\delta_{n_{\rho_1} n_{\rho_2}-1}]\delta_{s_1 s_2}\delta_{m_1 m_2 - 1}, \tag{28}$$

The rest of procedures can be performed by the numerical calculations. Since two-center model allows to vary deformation coefficient the wave functions appropriate for the current work would correspond to the equilibrium deformation value.

## 2.3 Equilibrium deformation in macroscopic-microscopic approach

The primary step made to describe a nucleus behavior under minor deformations is widely presented by the liquid drop model. The Bethe-Weizsäcker mass formula serves as a rough base for the fission barrier estimation and, therefore, it also ought to describe pre-fission states in general. However, appearances of such particularities as deviations from the smooth mass dependence (especially double-humped fission barriers in some isomers [9]) required taking larger deformations and shell effects (shell closures) into account.

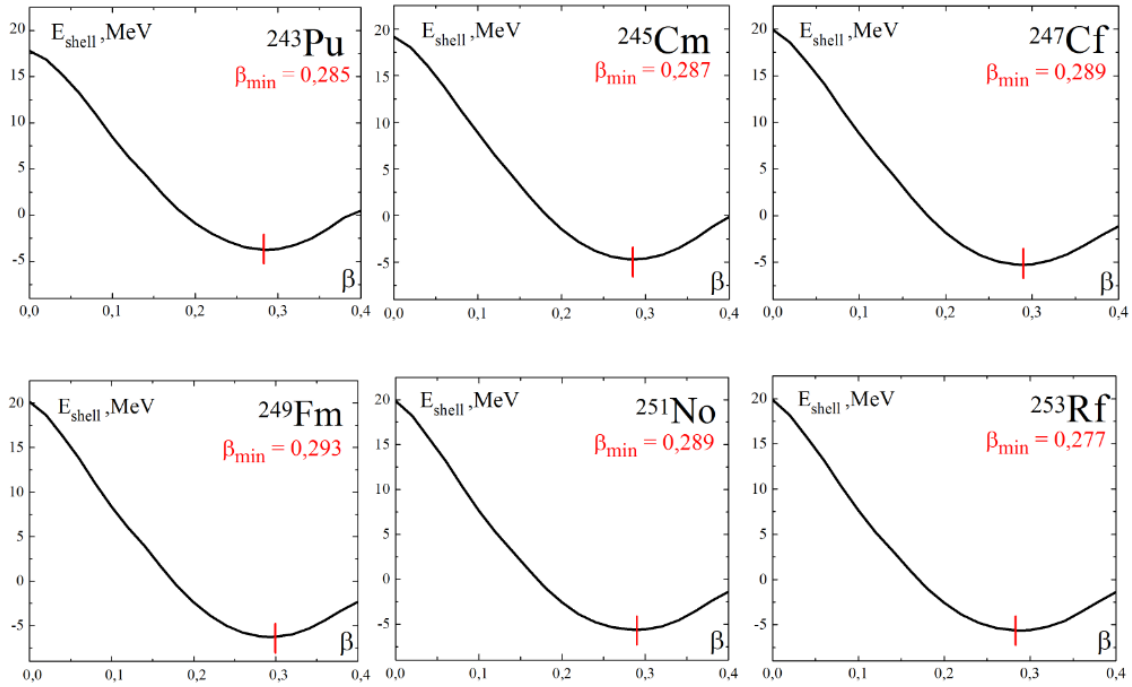


Figure 1: Total binding energy versus deformation parameter $\beta$ for the $^{243}$Pu, $^{245}$Cm, $^{247}$Cf, $^{249}$Fm, $^{251}$No and $^{253}$Rf isotopes.

Since the shell model by itself does not describe binding energies and fails to describe the general energy profile by considering motion of nucleons only in the vicinity of the Fermi energy, it was rather convenient to combine both the liquid drop model and the shell model. Such unification was performed by the Strutinski shell correction procedure [10]. It assumes this shell correction in a form of oscillatory addition to be inserted in the liquid drop bunding energy:

$$W_{tot} = W_{osc} + W_{LDM}. \tag{29}$$

These oscillations are firmly related to the shell ans subshell closures appearances and have the maxima on magic nuclei. This relation can also be enlarged if one operates in terms of shell model density levels. The oscillations can be understood if the average level density which would be responsible of the smooth $\tilde{W}_{sh}$ is introduced. Hence, the total energy can be presented as:

Table 1: Selected properties of investigated isotopes obtained by using TCSHM.

| | Isotope | | | | | |
|---|---|---|---|---|---|---|
| Parameter | $^{243}$Pu | $^{245}$Cm | $^{247}$Cf | $^{249}$Fm | $^{251}$No | $^{253}$Rf |
| $\beta_{min}$ | 0,285 | 0,287 | 0,289 | 0,293 | 0,289 | 0,277 |
| $(E_F)_n$, MeV | 49,674 | 49,544 | 49,417 | 49,299 | 49,149 | 48,966 |
| $\Delta_n$, MeV | 0,469 | 0,464 | 0.459 | 0.471 | 0.469 | 0.472 |
| $\Theta^{odd}$, MeV$^{-1}$ | 80,128 | 82,248 | 81,907 | 77,761 | 74,135 | |
| $\Theta^{even}$, MeV$^{-1}$ | 67,355 | 69,824 | 68,181 | 65,217 | | |

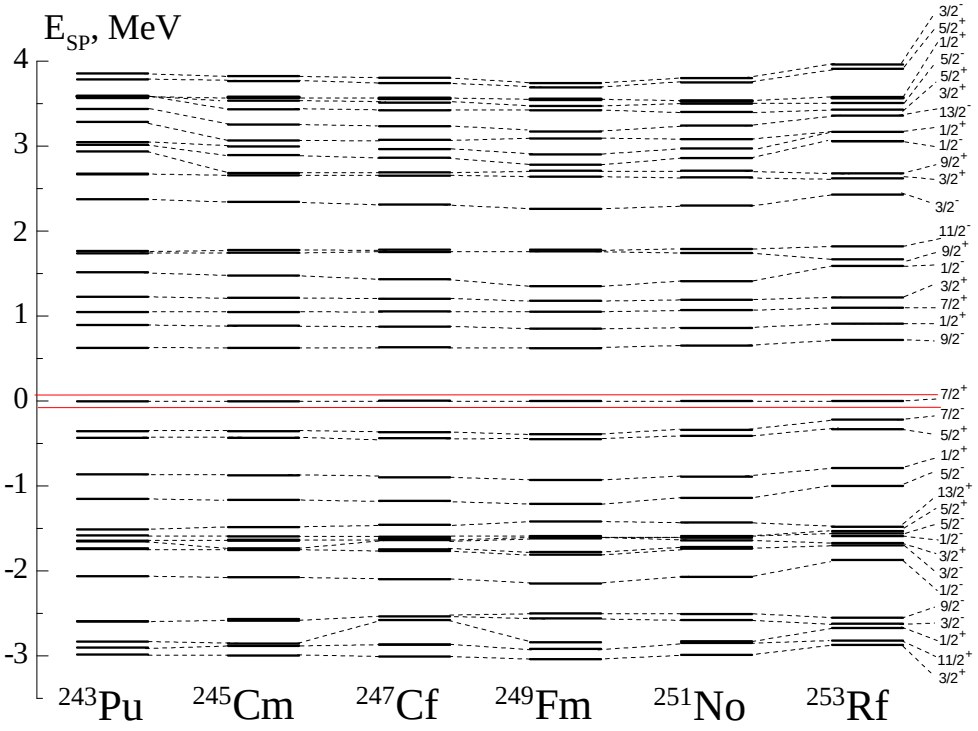


Figure 2: Spectra of neutron single-particle energies for the $^{243}$Pu, $^{245}$Cm, $^{247}$Cf, $^{249}$Fm, $^{251}$No and $^{253}$Rf isotopes.

$$W_{tot} = W_{LDM} + W_{sh} - \tilde{W}_{sh} = W_{LDM} + W_{sh} = W_{LDM} + \int_{-\infty}^{\lambda} \varepsilon g(\varepsilon) d\varepsilon - \int_{-\infty}^{\tilde{\lambda}} \varepsilon \tilde{g}(\varepsilon) d\varepsilon, \tag{30}$$

where $g(\varepsilon)$ and $g(\tilde{\varepsilon})$ are level density and smoothed level densities. In the present paper TCSHM program in $fortran$ was applied in order to calculate two-center single-particle states $\Phi_K^i$ at the equilibrium deformation $\beta$. In its turn these deformations were previously determines as $\beta_{min}$ which would correspond to the minima of shell corrections dependencies versus deformation (see Figure 1) as these minima almost coincide with those of total energy. The Fermi energies $(E_F)_n$, energy gaps $\Delta_n$ for these isotopes were determined as well (see Table 1). The spectra of single-particle energies with respect to the Fermi energy as a zero are presented on Figure 2.

According to The Bardeen-Cooper-Schrieffer theory the single-particle configurations in odd systems can be described in terms of the Bogolubov quasi-particles [2]. Therefore the single-particle spectra serve as a canvas for the quasi-particles excitations. These excitation energies can be presented in the form:

$$\varepsilon_k^Q = \sqrt{(\varepsilon_k^{SP} - E_F)^2 + \Delta^2}, \tag{31}$$

where $\varepsilon_k^{SP}$ are single-particle energies obtained in the framework of TCSHM, $\Delta^2$ and $E_F$ used in the calculation are mentioned in Table 1.

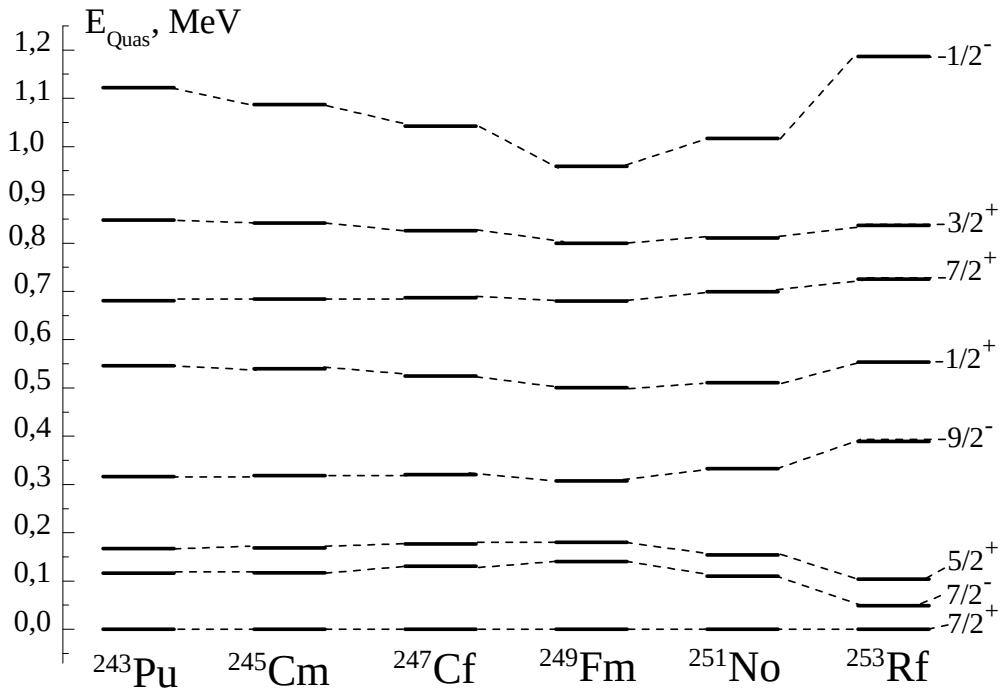


Figure 3: Spectra of neutron quasi-particle energies the $^{243}$Pu, $^{245}$Cm, $^{247}$Cf, $^{249}$Fm, $^{251}$No and $^{253}$Rf isotopes.

# 3 Realization

Whole procedure of taking the Coriolis interaction into account was performed in *Wolfram Mathematica* TCSHM program as an additional section (set of cells).

Since such essential parameters as $A, Z$,mass asymmetry, deformations of nuclear fragments, distance to the center of the first and second fragments, parameters of the TCSHM potential (i.e. all required TCSHM model parameters) were initially inserted in the TCSHM program, the rest to be set were local frame parameters as:

*zero = A - Z*
*lim = -40*
*Inert = 67*
*J = 7/2*
*fin = 40*

Where *zero* denotes the closest to the Fermi energy level,*Inert* is a moment of inertia,*J* is an *I* value, and *lim*,*f1* and *fin* are required to determine the number of levels under investigation below and above the Fermi level:

*H = Table[0, n1, 1, fin, n2, 1, fin];*

Henceforth *strv3[[]]* denotes different wave components with the same *K* value and TCSHM energy *energy0*.Therefore the procedure (19) will be rewritten as:

*Do*[{ *Do*[{
*K1 = Abs*[*strv3*[*zero + lim + 2*n1*][[*1, 4*]] + *strv3*[*zero +lim +2*n1*][[ *1, 5*]]],
*K2 = Abs*[*strv3*[*zero + lim + 2*n2*][[*1, 4*]] + *strv3*[*zero +lim +2*n2*][[ *1, 5*]]],
*N1 = zero + lim + 2*n1,*
*N2 = zero + lim + 2*n2,*
*If*[$(K1 > J) \| (K2 > J)$, *H*[[*n1, n2*]] = *energy0*[[*N1*]] *DF*[*N1, N2*] + $(J * (J + 1) - (K1)^2)/2/Inert*DF[N1, N2]$,{
*If*[$K1 == K2$, *H*[[*n1, n2*]] = *energy0*[[*N1*]] *DF*[*N1, N2*] + $(J * (J + 1) - (K1)^2)/2/Inert*DF[N1, N2]+$
$(-1)^(J + K1)*MatTot[N1, N2 + 1] * (-1/2/Inert) * (J + 1/2)/2*DF[K1, 1/2]+$
$(-1)^(J + K1)*MatTot[N1 + 1, N2] * (-1/2/Inert) * (J + 1/2)/2*DF[K1, 1/2]$, *None*],

Here *MatTot[]* is $\langle \Phi^i_{\frac{1}{2}} | J_+ | \Phi^i_{-\frac{1}{2}} \rangle$.

*If*[$K2 - K1 == 1$,
*H*[[*n1, n2*]] = $Sqrt[(J + K2) * (J - K1)]*$(*MatTot*[*N2, N1*] - *MatTot*[*N1 + 1, N2 + 1*]) $* (-1/2/Inert)/2$, *None*],
*If*[$K1 - K2 == 1$,
*H*[[*n1, n2*]] = $Sqrt[(J + K1) * (J - K2)]*$(*MatTot*[*N1, N2*] - *MatTot*[*N2 + 1, N1 + 1*]) $* (-1/2/Inert)/2$, *None*],
*n2++*}, {*n2, 1, fin*}], *n1++*}, {*n1, 1, fin*}]

Then the eigenvalues and eigenvectors are determined by:

{*eng, vct*} = *Eigensystem*[*H*];

It is followed by the renormalization procedure (*engN[[]]* and *vctN[[]]* will be recalled by the same number as *energy0[[]]*):

*Hindex = Table[zero + lim + 2*n1, {n1, 1, fin}];*
*engN = Table[0, [n1, 1, Hindex[[Length[Hindex]]]{];*
*vctN = Table[ 0, {n1, 1, Hindex[[Length[Hindex]]]{, {n1,1,Hindex[[Length[Hindex]]]{;*
*Do[{engN[[Hindex[[n1]]]] = eng[[fin - n1 + 1]]} , {n1, 1, fin}]*
*Do[{vctN[[Hindex[[n1]]]] = vct[[fin - n1 + 1]]} , {n1, 1, fin}]*

The different $K$-admixtures can be represented by their contributions with corresponding weight (in percent):

*Nm = 149; Sum[ Chop[vctN[[Nm, k]], 0.01] f[zero + lim + 2 k, strv3[Hindex[[k]]][[1, 4]], strv3[zero + lim + 2 k[]]1, 5]]], {k, 1, Length[vctN[[Nm]]]}]*

Energy of each level is recalled by:

*engN[[]]*

As the result of each run for the different $I$ values one obtains the set of single-particle energies in the vicinity of the Fermi energy for the selected isotone.

# 4 Results

In the frame of chosen theoretical approach the decopling factors (i.e. $\langle \Phi^i_{\frac{1}{2}} | J_+ | \Phi^i_{-\frac{1}{2}} \rangle$)for each of isotones were calculated and listed in Table 2.

Table 2: Decoupling factors of investigated isotopes obtained by using TCSHM.

| Decoupling factors | | | | | |
|---|---|---|---|---|---|
| $^{243}$Pu | $^{245}$Cm | $^{247}$Cf | $^{249}$Fm | $^{251}$No | $^{253}$Rf |
| -1,685 | -1,683 | -1,682 | -1,679 | -1,682 | -1,689 |

As long as the internal structures of these nuclei are quite similar (that was also proved by the close deformation parameters $\beta$) the corresponding decoupling factors do not vary significantly. They cause the noticeable downward shift of $\frac{1}{2}^+$ state (see Figure 4 and Figure 5) by 10-20 keV. Their values depend only on the calculated by TCSHM wave functions, thus they do not reflect the the consequences of some moment of inertia values deviations. However such deviations may be crucial for the general order of single-particle states as the moment of inertia minimization evokes the Coriolis interaction amplitude increase. Figure 4 and Figure 5 represent the spectra obtained for $\Theta^{even}$ which correspond to the independent even-even core and particle approach. Indeed, the mathematical background assumes them to be independent, so such choice of $\Theta$ would correlate with underlying calculations. Still this assumption is far from the genuine nature and

an another limit of rigidly bound core and particle was taken into account as well. $\Theta^{odd}$ were calculated on the base of experimental ground state $\frac{7}{2}^+$ band for the selected nuclei in contras to $Theta^{even}$ obtained for the corresponding $(Z, N-1)$ nuclei. Since the experimental data on $^{251}$No and $^{253}$Rf are quite scarce the $\Theta$ values were extrapolated by known values for lighter nuclei.

The less of more reliable criteria of proper $\Theta$ selection can be chosen on the base of calculated and experimental bands comparison. For such procedure the ground state $\frac{7}{2}^+$ band was selected as long as it was measured in numerous experiments with an appropriate precision for super-heavy nuclei thus being optimally reliable. These bands for the selected nuclei are plotted on Figure 6. The smooth non wave-like (parabolic) behavior of those points to the weak Coriolis mixing for $K = \frac{7}{2}$. The experimental points fit the calculated curves with a slight deviation in large $I$ which might be eliminated by $\Theta$ selection. As the reference fitting points $I = \frac{7}{2}$ and $I = \frac{11}{2}$ were selected. The approximate values of fitted $\Theta*$ are listed in Table 3. These values imply that the internal structure of each nuclei is closer to the strong limit rather

Table 3: Moments of inertia of investigated isotopes.

| Moments of inertia, $MeV^{-1}$ | | | |
|---|---|---|---|
| $^{243}$Pu | $^{245}$Cm | $^{247}$Cf | $^{249}$Fm |
| 77 | 79 | 78 | 76 |

than to the limit of independent constituents. However the blocking effect (as the way of taking pairing into account directly) would probably cause the significant increase of moment of inertia. Thus the limit of independent core and particle would approach that of the rigid system.

On the other hand, the $\frac{1}{2}^+$ band is an object of particular interest as well since the Coriolis interaction was predicted to influence significantly on it. These bands are presented on Figure 7 for all selected super-heavy nuclei. The rotational parabolic behavior is disrupted by the Coriolis mixing, hence the serrated behavior of each curve. The experimental data for the $\frac{1}{2}^+$ band are not available for the majority of the investigated nuclei. However even the available data (for $^{243}$Pu and $^{245}$Cm) are quite doubtful. For $^{243}$Pu the experimental points for $I = \frac{3}{2}$ and $I = \frac{5}{2}$ reveal a reverse tendency as compared with the calculated one. The actual essence of these states differ from those of pure $\frac{1}{2}^+$ band components. These states may even present a mixture of states with the corresponding quantum numbers. Almost the same can be traced for the $^{245}$Cm isotope: the experiential data (red points, starting with 0,355 MeV) reveal ladder-like tendency with no explicit maxima and minima. Moreover they disperse with the calculated ones over all range. Such discrepancies allow us to doubt in experimental data pureness. But for the second $\frac{1}{2}^+$ measured band (blue points, starting with 0,740 MeV) these discrepancies are less significant, though the Coriolis mixing is still reduced. This experimental band has an additional $\frac{1}{2}^-$ (0,913 MeV) band thus forming a doublet with it typical for octopole deformation. Indeed such kind of deformation is ought to be inherent in the investigated mass ($A$) range. As the result the week Coriolis effect and an absence of a doublet itself serve as reason for considering $\frac{1}{2}^+$ band to be first observed $\frac{1}{2}^+$ rotational band, as the first one to be essentially misunderstood. Probably it does actually contain the rotational band but rather based on $\frac{3}{2}^+$.

Taking the Coriolis interaction into account would allow to obtain the probabilities of E2 transitions from the $\frac{1}{2}^+$ excited state to the $\frac{5}{2}^+$ excited state as well. All underlying calculations are presented in Appendix B and the probabilities ($s^{-1}$) themselves are taken as [3]:

$$T = 1,223 * 10^9 E^5 * B(E2). \tag{32}$$

The lifetimes obtained for each isotone are listed in Table 4. Hence the $\frac{1}{2}^+$ state in $^{249}$Fm has the largest

Table 4: $E2$ transition probabilities and $\frac{1}{2}^+$ lifetimes for the investigated isotopes.

| | $^{243}$Pu | $^{245}$Cm | $^{247}$Cf | $^{249}$Fm | $^{251}$No | $^{253}$Rf |
|---|---|---|---|---|---|---|
| B(E2), $e^2$fm$^4$ | 0,821 | 0,715 | 0,754 | 0,644 | 0,890 | 0,738 |
| lifetime, $\mu$s | 0,35 | 0,46 | 0,51 | 1,12 | 0,34 | 0,16 |

lifetime mostly due to the narrowest energy gap between the initial and final states.This gap tend to increase for $^{253}$Rf thus decreasing the lifetime. This $\frac{1}{2}^+$ state for $^{253}$Rf is quite far from being the isomeric state as it was predicted experimentally mostly due to the energy gap increase despite the increasing $B(E2)$ value.

# 5 Conclusions

In the present paper the $N$-odd $Z$-even super-heavy nuclei such as $^{243}$Pu, $^{245}$Cm, $^{247}$Cf, $^{249}$Fm,$^{251}$No, and $^{253}$Rf were investigated in the framework of rotor-plus-particle approach. As the intermediate step the two-center shell model was used in order to obtain the single-particle spectra henceforth being converted to the quasi-particle spectra.On the base of these spectra the Coriolis interaction was inserted to obtain the shifted spectra and to trace the mixing of states (especially $\frac{1}{2}^+$) due to this interaction. The calculated results were compared with the experimental data and some conclusions on the reliability of experimental data were made. The calculated data were used as the base for $\frac{1}{2}^+$ lifetimes estimations. During this work I was able to treat the macroscopic-microscopic in its actual applications to the real isotonic chain. The base of TCSHM especially was studied as well. I have also received an experience of the mathematical realization of theoretical framework via the technical facilities. This project is about to be continued and extended on other isotonic chains with blocking effect and surface vibrations taken into account.

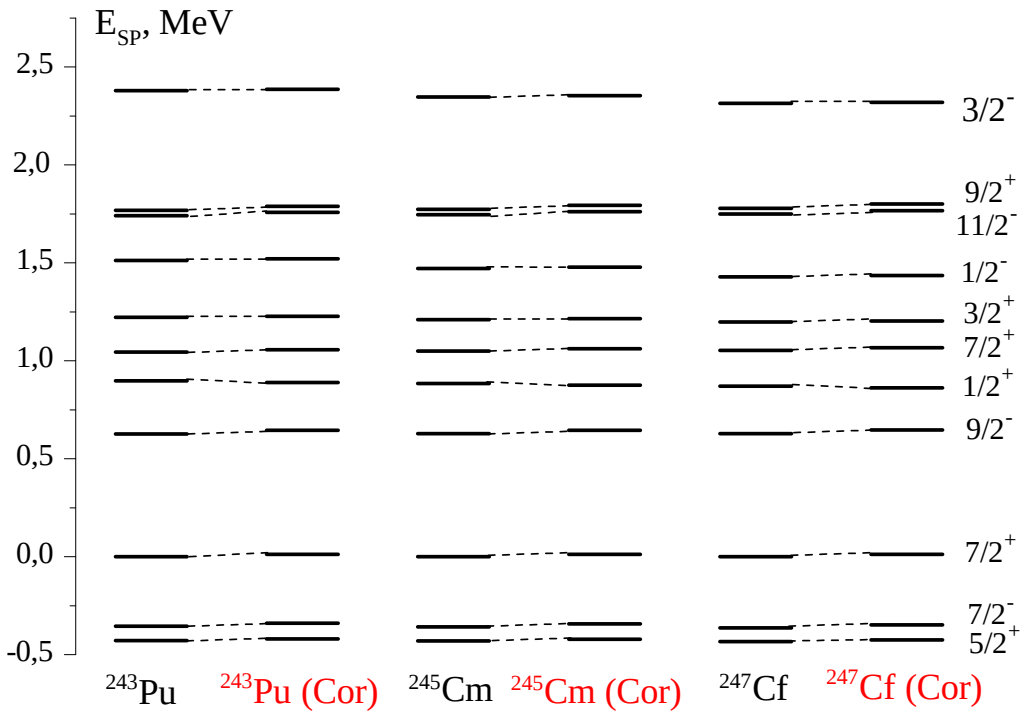


Figure 4: Spectra of neutron single-particle energies the $^{243}$Pu, $^{245}$Cm, and $^{247}$Cf isotopes.

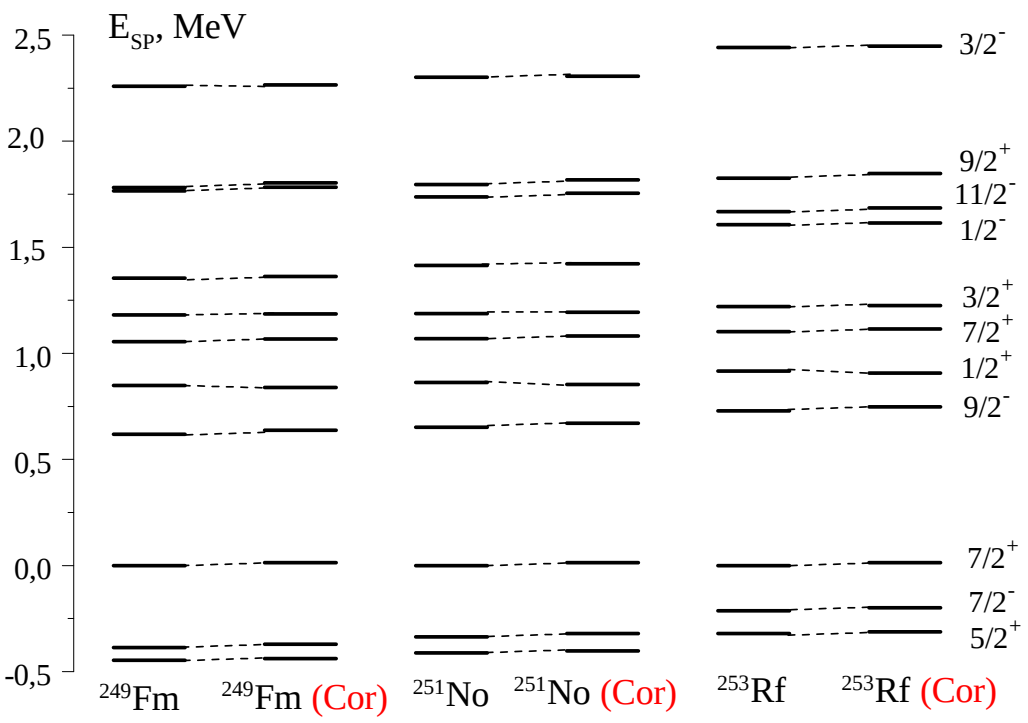


Figure 5: Spectra of neutron single-particle energies the $^{249}$Fm, $^{251}$No, and $^{253}$Rf isotopes.

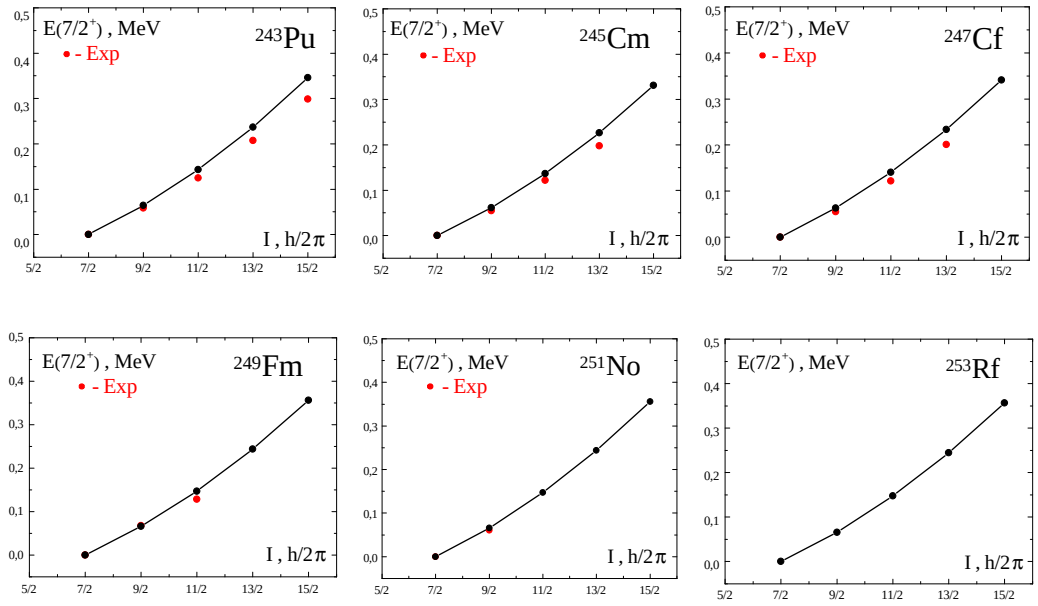


Figure 6: $K = 7/2^+$ band for $^{243}$Pu, $^{245}$Cm, $^{247}$Cf, $^{249}$Fm, $^{251}$No and $^{253}$Rf isotopes.

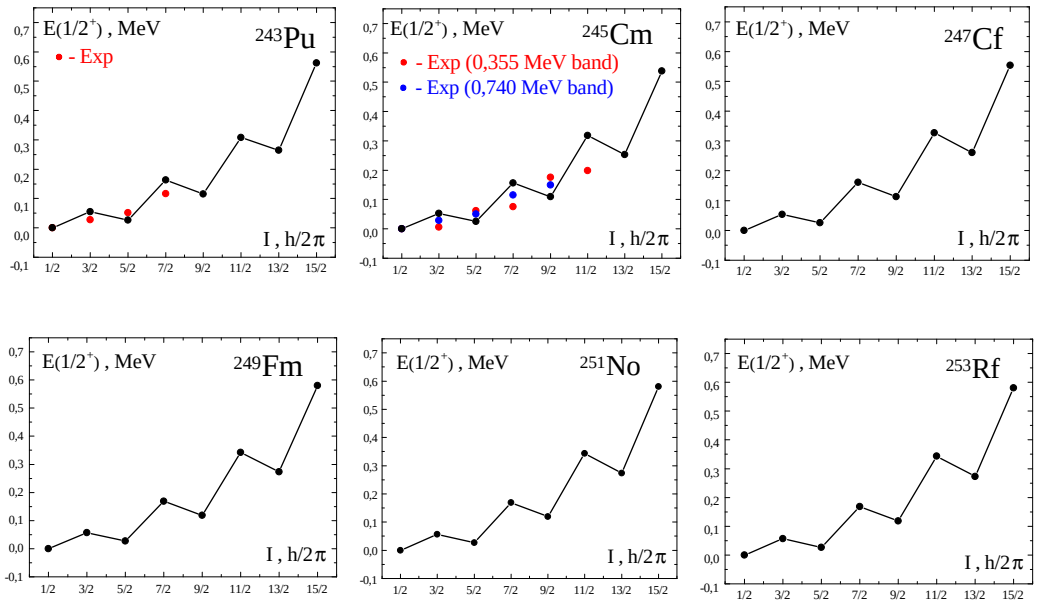


Figure 7: $K = 1/2^+$ band for $^{243}$Pu, $^{245}$Cm, $^{247}$Cf, $^{249}$Fm, $^{251}$No, and $^{253}$Rf isotopes.

# References


[1] J. Maruhn, W. Greiner, Z. / Physik 251., p.431–457. (1972).

[2] P. Ring, P. Schuck / The Nuclear Many-Body Problem, Vol.1, (Springer-Verlag, New-York Ink. 1995)

[3] P. Ring, P. Schuck / The Nuclear Many-Body Problem, Vol.1, (Springer-Verlag, New-York Ink. 1995)

[4] A. Bohr, B. R. Mottelson / Nuclear structure, Vol.2, (World Scientific Publishing Co, Singapore, 1998)

[5] W. Greiner, J.A. Maruhn / Nuclear models, (Springer-Verlag, Berlin, 1995)

[6] J. M. Eisenberg, W. Greiner / Nuclear Theory, Vol. 3, Microscopic Theory of the Nucleus, (Amsterdam, 1972).

[7] D.A. Varshalovich, A.N. Moskalev, V.K. Kherson / Quantum theory of angular momentum (Publishing house ”Science”, Leningrad Department, Leningrad, 1975) [in Russian].

[8] V. G. Soloviev / Atomic Nuclear Theory: Nuclear Models (Moscow, 1981) [in Russian].

[9] S. M. Polikanov et al. / Exp. Theor. Phys., 42, 1464 (1962)

[10] V. M. Strutinsky / Nucl. Phys. A95, 420 (1967)

[11] R.-D. Herzberg, P. T. Greenlees / Progress in Particle and Nuclear Physics, 61, 674-720 (2008)

[12] F. G. Kondev, G. D. Dracoulis, T. Kibedi / Atomic Data and Nuclear Data Tables, 103-104, 50-105 (2015)

[13] Evaluated Nuclear Structure Data File. Brookhaven, National Nuclear Data Center. http://ie.lbl.gov/ensdf/

[14] G. Ardison, et al., Radiochim. / Acta 78 15 (1997)

[15] T. H. Braid, et al. / Phys. Rev. C 4, 247 (1971)

[16] Y. A. Akovali / Nucl. Data Sheets 102, 515 (2004)

[17] A. Lopez-Martens, et al. / Eur. Phys. J. A 32, 245 (2007)

[18] F. P. Hessberger, et al. / Eur. Phys. J. A 30, 561 (2006)

# A Matrix elements $H_{K_iK_j}$ and decoupling parameter

In order to obtain matrix elements of the Hamiltonian:

$$H = H_{intr} + \frac{I^2 - K^2}{2\Theta} - \frac{I_+J_- + I_-J_+}{2\Theta} \tag{A.1}$$

one ought take into account orthogonality of Wigner functions and[3]

$$I_\pm D^I_{MK}(\Omega) = \sqrt{(I \pm K)(I \mp K + 1)} D^I_{MK\mp1}(\Omega). \tag{A.2}$$

Thus, for diagonal elements $K_i = K_j = K$ one will receive:

$$\langle \sqrt{\frac{2I+1}{16\pi^2}} \left( D^I_{MK}(\Omega)\Phi^i_K + (-1)^(I+K) D^I_{M-K}(\Omega)\Phi^i_{-K} \right) |H| \sqrt{\frac{2I+1}{16\pi^2}} \left( D^I_{MK}(\Omega)\Phi^i_K + (-1)^(I+K) D^I_{M-K}(\Omega)\Phi^i_{-K} \right) \rangle =$$

$$= \epsilon^I_K + \frac{I(I+1) - K^2}{2\Theta} + \frac{1}{2}\left(-\frac{1}{2\Theta}\right)\left(\frac{2I+1}{8\pi^2}\right) \sqrt{(I+K)(I-K+1)} (\langle D^I_{MK}|D^I_{MK-1}\rangle \langle \Phi^i_K|J_-\Phi^i_K\rangle +$$

$$+(-1)^{I+K} \langle D^I_{MK}|D^I_{M-K+1}\rangle \langle \Phi^i_K|J_+\Phi^i_{-K}\rangle + (-1)^{I+K} \langle D^I_{M-K}|D^I_{MK-1}\rangle \langle \Phi^i_{-K}|J_-\Phi^i_K\rangle + \langle D^I_{M-K}|D^I_{M-K+1}\rangle \langle \Phi^i_{-K}|J_+\Phi^i_{-K}\rangle) +$$

$$\frac{1}{2}\left(-\frac{1}{2\Theta}\right)\left(\frac{2I+1}{8\pi^2}\right) \sqrt{(I-K)(I+K+1)} (\langle D^I_{MK}|D^I_{MK+1}\rangle \langle \Phi^i_K|J_+\Phi^i_K\rangle + (-1)^{I+K} \langle D^I_{MK}|D^I_{M-K-1}\rangle \langle \Phi^i_K|J_-\Phi^i_{-K}\rangle +$$

$$+ \langle D^I_{M-K}|D^I_{M-K-1}\rangle \langle \Phi^i_{-K}|J_-\Phi^i_{-K}\rangle + (-1)^{I+K} \langle D^I_{M-K}|D^I_{MK+1}\rangle \langle \Phi^i_{-K}|J_+\Phi^i_K\rangle). \tag{A.3}$$

The only value of K which would provide us with nonzero items is $K = \frac{1}{2}$ ($K = -K + 1$ and $-K = K - 1$ combinations, $K$ has positive sign). So, $H_{KK}$ will be reduced for $K \neq \frac{1}{2}$:

$$H_{KK} = \epsilon^I_K + \frac{I(I+1) - K^2}{2\Theta}, \tag{A.4}$$

And for $K = \frac{1}{2}$:

$$H_{KK} = \epsilon^I_K + \frac{I(I+1) - K^2}{2\Theta} + \frac{1}{2}\left(-\frac{1}{2\Theta}\left(I + \frac{1}{2}\right)\left[\langle \Phi^i_K|J_+|\Phi^i_{-K}\rangle + \langle \Phi^i_{-K}|J_-|\Phi^i_K\rangle\right]. \tag{A.5}$$

For $H_{KK+1}$ case one obtain:

$$\frac{2I+1}{16\pi^2} \langle D^I_{MK}(\Omega)\Phi^i_K + (-1)^(I+K) D^I_{M-K}(\Omega)\Phi^i_{-K}|H|D^I_{MK+1}(\Omega)\Phi^i_{K+1} + (-1)^(I+K+1) D^I_{M-K-1}(\Omega)\Phi^i_{-K-1}\rangle .$$

Here the only combinations which leave nonzero items are $K = K$ and $-K = -K$ (the first part of these equalities is from bra vector, the latter would correspond to ket vector). Thus:

$$H_{KK+1} = \frac{1}{2}\left(\frac{1}{2\Theta}\right) \sqrt{(I+K+1)(I-K)} \left[\langle \Phi^i_K|J_-|\Phi^i_{K+1}\rangle - \langle \Phi^i_{-K}|J_+|\Phi^i_{-K-1}\rangle\right]. \tag{A.6}$$

Exactly the same result will be symmetrically obtained for $H_{K+1K}$ as long as it provides with two nonzero combinations $K+1 = K+1$ and $-K-1 = -K-1$. For the rest of $K_i$ and $K_j$ combinations in matrix elements these $K$ will be zero or negative and since $K$ is positive the corresponding matrix elements will be $H_{K_iK_j} = 0$.

# B Matrix elements of $Q_{2\mu}$ operator and $B(E2)$

Nuclear surface vibrations can be represented in the following form (laboratory system)[2]:

$$R(\theta,\phi,t) = R_0\left(1+\sum_{\lambda,\mu}(-1)^{\mu}\alpha_{\lambda-\mu}(t)Y_{\lambda\mu}(\theta,\phi)\right). \tag{B.1}$$

Applying the relations via the Euler angles and eliminating time dependence [7]:

$$\alpha_{\lambda\mu} = \sum_{\nu} D^{\lambda*}_{\nu\mu}(\Omega)a_{\lambda\mu}, \tag{B.2}$$

$$Y_{\lambda\mu}(\theta,\phi) = \sum_{\nu} D^{\lambda*}_{\nu\mu}(\Omega)Y_{\lambda\mu}(\theta',\phi'), \tag{B.3}$$

allows to switch laboratory framework to the internal one and take only quadrupole deformations into account:

$$R(\theta',\phi') = R_0\left(1+\sum_{\lambda,\mu}(-1)^{\mu}a_{\lambda-\mu}Y_{\lambda\mu}(\theta',\phi')\right), \tag{B.4}$$

and, finally, insert such new variables as $\beta$ and $\gamma$ deformations: $a_{20} = \beta\cos(\gamma)$, $a_{2\pm1} = 0$, and $a_{2\pm2} = \frac{\sqrt{2}}{2}\beta\sin(\gamma)$. The $Q_{\lambda\mu}$ operator itself can be represented for the inner even-even core and particle as:

$$Q_{\lambda\mu} = \sum_{i=1}^{A} e_{eff}r_i^{\lambda}Y_{\lambda\mu}*(\theta_i,\phi_i) = \sum_{i=1}^{A-1} e_{eff}r_i^{\lambda}Y_{\lambda\mu}*(\theta_i,\phi_i) + e_{eff}r_A^{\lambda}Y_{\lambda\mu}*(\theta_A,\phi_A), \tag{B.5}$$

$$Q_{2\mu} == \sum_{i=1}^{A-1} e_{eff}r_i^{2}Y_{2\mu}*(\theta_i,\phi_i) + e_{eff}r_A^{2}Y_{2\mu}*(\theta_A,\phi_A), \tag{B.6}$$

where $e_{eff}$ is an effective charge for proton of neutron.Meanwhile the wave function can be represented by:

$$\Psi_{tot} = \sum_{K}\psi_{S\,lat.det.}(\vec{r}_1,\vec{r}_2,...,\vec{r}_{A-1})g(\beta,\gamma)\,|KLM\rangle =$$

$$= \sum_{K}|core.p\rangle\, g(\beta,\gamma)\sqrt{\frac{2I+1}{16\pi^2}}\left(D^{I}_{MK}(\Omega)\phi^{i}_{K} + (-1)^{I+K}D^{I}_{M-K}(\Omega)\phi^{i}_{-K}\right). \tag{B.7}$$

Splitting $Q_{2\mu}$ into the core part $Q^1_{2\mu}$ and particle dependent part $Q^2_{2\mu}$ one may obtain for the first part:

$$A_1 = \langle core.p|Q^1_{2\mu}|core.p\rangle = e_{eff}\frac{3ZR_0^2}{4\pi}\alpha_{2\mu}* = e_{eff}\frac{3ZR_0^2}{4\pi}\sum_{\nu}D^{2}_{\mu\nu}(\Omega)(-1)^{\mu}a_{2-\mu}, \tag{B.8}$$

$$A_2 = \langle g(\beta,\gamma)|A_1|g(\beta,\gamma)\rangle = e_{eff}\frac{3ZR_0^2}{4\pi}D^{2}_{\mu0}(\Omega) < \beta >, \tag{B.9}$$

Taking the form of integrals including three Wigner functions in [7] one obtains:

$$\langle I_fM_fK_f|A_2|I_iM_iK_i\rangle = \sum_{K_f}\sum_{K_i}a_{K_f}*a_{K_i}e_{eff}\frac{3ZR_0^2}{4\pi}(\Omega) < \beta > \sqrt{\frac{2I_f+1}{16\pi^2}}\sqrt{\frac{2I_i+1}{16\pi^2}}\otimes$$

$$\otimes \int \left(D^{I_f}_{MK_f} * (\Omega)\phi_{K_f} * + (-1)^{I_f+K_f} D^{I_f}_{M-K_f} * (\Omega)\phi_{-K_f} *\right) D^2_{\mu 0}(\Omega) \left(D^{I_i}_{MK_i} * (\Omega)\phi_{K_i} * + (-1)^{I_i+K_i} D^{I_i}_{M-K_i} * (\Omega)\phi_{-K} *\right) d\Omega dq =$$

$$\sum_{K_f} \sum_{K_i} a_{K_f} * a_{K_i} e_{eff} \frac{3ZR_0^2}{4\pi}(\Omega) < \beta > \sqrt{\frac{2I_f+1}{16\pi^2}} \sqrt{\frac{2I_i+1}{16\pi^2}} [\int D^{I_f}_{MK_f} * (\Omega) D^2_{\mu 0}(\Omega) D^{I_i}_{MK_i} * (\Omega) d\Omega \langle \phi_{K_f} | \phi_{K_i} \rangle +$$

$$+ (-1)^{I_f+K_f} \int D^{I_f}_{M-K_f} * (\Omega) D^2_{\mu 0}(\Omega) D^{I_i}_{MK_i} * (\Omega) d\Omega \langle \phi_{-K_f} | \phi_{K_i} \rangle + (-1)^{I_i+K_i} \int D^{I_f}_{MK_f} * (\Omega) D^2_{\mu 0}(\Omega) D^{I_i}_{M-K_i} * (\Omega) d\Omega \langle \phi_{K_f} | \phi_{-K_i} \rangle +$$

$$(-1)^{I_f+K_f+I_i+K_i} \int D^{I_f}_{M-K_f} * (\Omega) D^2_{\mu 0}(\Omega) D^{I_i}_{M-K_i} * (\Omega) d\Omega \langle \phi_{-K_f} | \phi_{-K_i} \rangle] = \quad (B.10)$$

$$\sum_{K_f} \sum_{K_i} a_{K_f} * a_{K_i} e_{eff} \frac{3ZR_0^2}{4\pi}(\Omega) < \beta > \sqrt{\frac{2I_f+1}{16\pi^2}} \sqrt{\frac{2I_i+1}{16\pi^2}} \frac{8\pi^2}{2I_f+1} [C^{I_f M_f}_{I_i M_i 2\mu} C^{I_f K_f}_{I_i K_i 20} \langle \phi_{K_f} | \phi_{K_i} \rangle +$$

(

$$+ (-1)^{I_f+K_f} C^{I_f M_f}_{I_i M_i 2\mu} C^{I_f - K_f}_{I_i K_i 20} \langle \phi_{-K_f} | \phi_{K_i} \rangle + (-1)^{I_i+K_i} C^{I_f M_f}_{I_i M_i 2\mu} C^{I_f K_f}_{I_i - K_i 20} \langle \phi_{K_f} | \phi_{-K_i} \rangle +$$

$$(-1)^{I_f+K_f+I_i+K_i} C^{I_f M_f}_{I_i M_i 2\mu} C^{I_f - K_f}_{I_i - K_i 20} \langle \phi_{-K_f} | \phi_{-K_i} \rangle] =$$

$$\sum_{K_f} \sum_{K_i} a_{K_f} * a_{K_i} e_{eff} \frac{3ZR_0^2}{4\pi}(\Omega) < \beta > \frac{1}{2} \frac{\sqrt{2I_i+1}}{\sqrt{2I_f+1}} C^{I_f M_f}_{I_i M_i 2\mu} [C^{I_f K_f}_{I_i K_i 20} (\langle \phi_{K_f} | \phi_{K_i} \rangle + (-1)^{2I_f - 2 + K_f + K_i} \langle \phi_{-K_f} | \phi_{-K_i} \rangle) +$$

$$+ C^{I_f - K_f}_{I_i K_i 20} ((-1)^{I_f+K_f} \langle \phi_{-K_f} | \phi_{K_i} \rangle + (-1)^{I_f - 2 + K_i} \langle \phi_{K_f} | \phi_{-K_i} \rangle)], \quad (B.11)$$

For the second part for a particle one obtains:

$$B_1 = \langle g(\beta, \gamma) core.p | Q^2_{2\mu} | g(\beta, \gamma) core.p \rangle = \delta_{K_f K_i}, \quad (B.12)$$

$$\langle I_f M_f K_f | B_1 | I_i M_i K_i \rangle = \sum_{K_f} \sum_{K_i} a_{K_f} * a_{K_i} e_{eff} \sqrt{\frac{2I_f+1}{16\pi^2}} \sqrt{\frac{2I_i+1}{16\pi^2}} \int \left(D^{I_f}_{MK_f} * (\Omega)\phi_{K_f} * + (-1)^{I_f+K_f} D^{I_f}_{M-K_f} * (\Omega)\phi_{-K_f} *\right) \otimes$$

$$\otimes D^2_{\mu 0}(\Omega) r_A^2 Y_{20} * (\theta_A, \phi_A) \left(D^{I_i}_{MK_i} * (\Omega)\phi_{K_i} * + (-1)^{I_i+K_i} D^{I_i}_{M-K_i} * (\Omega)\phi_{-K} *\right) d\Omega dq =$$

$$= \sum_{K_i} a_{K_f} * a_{K_i} e_{eff} \frac{1}{2} \frac{\sqrt{2I_i+1}}{\sqrt{2I_f+1}} C^{I_f M_f}_{I_i M_i 2\mu} [C^{I_f K_f}_{I_i K_i 20} (\langle \phi_{K_f} | r_A^2 Y_{20} * (\theta_A, \phi_A) | \phi_{K_i} \rangle + (-1)^{2I_f - 2 + K_f + K_i} \langle \phi_{-K_f} | r_A^2 Y_{20} * (\theta_A, \phi_A) | \phi_{-K_i} \rangle) +$$

$$+ C^{I_f - K_f}_{I_i K_i 20} ((-1)^{I_f+K_f} \langle \phi_{-K_f} | r_A^2 Y_{20} * (\theta_A, \phi_A) | \phi_{K_i} \rangle + (-1)^{I_f - 2 + K_i} \langle \phi_{K_f} | r_A^2 Y_{20} * (\theta_A, \phi_A) | \phi_{-K_i} \rangle)], \quad (B.13)$$

The combination of (B.11) and (B.13) is a full matrix element for $Q_{2\mu}$ operator. Henceforth the reduced transition probability can be calculated as [6]:

$$B(J_i \to J_f) = \frac{1}{2J_i+1} \sum_{M_i, M_f, \mu} |\langle J_f M_f | Q_{2\mu} | J_i M_i \rangle|^2 = \frac{2J_f+1}{2J_i+1} |\langle f || Q_{2\mu} || i \rangle|^2, \quad (B.14)$$

and the reduced matrix element is given by the Wigner-Eckart theorem:

$$\langle J_f M_f | Q_{2\mu} | J_i M_i \rangle = C^{I_f M_f}_{I_i M_i 2\mu} \frac{\langle f || Q_{2\mu} || i \rangle}{2I_f+1}. \quad (B.15)$$